THE JOURNAL OF BIOLOGICAL CHEMISTRY VOL. 284, NO. 22, pp. 14949–14957, May 29, 2009

Stereospecificity of the Siderophore Pyochelin Outer Membrane Transporters in Fluorescent Pseudomonads*

Received for publication, January 28, 2009, and in revised form, March 4, 2009 Published, JBC Papers in Press, March 17, 2009, DOI 10.1074/jbc.M900606200

Françoise Hoegy[‡], Xiaoyun Lee[§], Sabrina Noel[‡], Didier Rognan[¶], Gaëtan L. A. Mislin[‡], Cornelia Reimmann[§], and Isabelle J. Schalk[‡1]

From the [‡]Métaux et Microorganismes, Chimie, Biologie, et Applications, CNRS-Université de Strasbourg, École Superieure de Biotechnologie Strasbourg, Boulevard Sébastien Brant, F-67413 Illkirch, Strasbourg, France, [§]Département de Microbiologie Fondamentale, Université de Lausanne, Bâtiment Biophore, Quartier UNIL-Sorge, CH-1015 Lausanne, Switzerland, and [¶]Département de Pharmacochimie de la Communication Cellulaire, CNRS-Université de Strasbourg, Faculté de Pharmacie 74, route du Rhin, 67401 Illkirch Graffenstaden Cedex, France

Pyochelin (Pch) and enantio-pyochelin (EPch) are enantiomer siderophores that are produced by *Pseudomonas aeruginosa* and *Pseudomonas fluorescens*, respectively, under iron limitation. Pch promotes growth of *P. aeruginosa* when iron is scarce, and EPch carries out the same biological function in *P. fluorescens*. However, the two siderophores are unable to promote growth in the heterologous species, indicating that siderophore-mediated iron uptake is highly stereospecific. In the present work, using binding and iron uptake assays, we found that FptA, the Fe-Pch outer membrane transporter of *P. aeruginosa*, recognized (K_d = 2.5 ± 1.1 nM) and transported Fe-Pch but did not interact with Fe-EPch. Likewise, FetA, the Fe-EPch receptor of *P. fluorescens*, was specific for Fe-EPch (K_d = 3.7 ± 2.1 nM) but did not bind and transport Fe-Pch. Growth promotion experiments performed under iron- limiting conditions confirmed that FptA and FetA are highly specific for Pch and EPch, respectively. When *fptA* and *fetA* along with adjacent transport genes involved in siderophore uptake were swapped between the two bacterial species, *P. aeruginosa* became able to utilize Fe-EPch as an iron source, and *P. fluorescens* was able to grow with Fe-Pch. Docking experiments using the FptA structure and binding assays showed that the stereospecificity of Pch recognition by FptA was mostly due to the configuration of the siderophore chiral centers C4″ and C2″ and was only weakly dependent on the configuration of the C4′ carbon atom. Together, these findings increase our understanding of the stereospecific interaction between Pch and its outer membrane receptor FptA.

To access iron, aerobic bacteria produce siderophores which form complexes with Fe^{3+} in the environment and deliver it via specific membrane transporters to the bacteria (1). The energy required for this process is provided by the proton motive force of the inner membrane by means of an inner membrane complex comprising TonB, ExbB, and ExbD (2, 3). Pyochelin (Pch),[2] which is the focus of this study, is produced as a secondary siderophore under iron limitation by almost all strains of *Pseudomonas aeruginosa* and some closely related bacteria (4–7). In pseudomonads, secondary siderophores (pyochelin, thioquinolobactin, etc.) are usually produced in smaller amounts, demonstrate lower iron affinity, and are rather simple molecules compared with pyoverdin (the main siderophore). It is hypothesized that under certain environmental or physiological conditions, secondary siderophores provide sufficient iron to the cell or fulfill functions other than iron sequestration (8). Pch was isolated for the first time from *P. aeruginosa* ATCC 15692 by Liu and Shokrani (9), and its structure was established later by Cox *et al.* (10) as (4′*R*,2″*R*,4″*R*)-2′-(2-hydroxyphenyl)-3″-methyl-4′,5′,2″,3″,4″,5″-hexahydro-[4′,2″]bithiazolyl-4″-carboxylic acid with three chiral centers located at C4′, C2″, and C4″ (see Fig. 1). Pch is synthesized by *P. aeruginosa* from salicylate and two molecules of cysteine via a thiotemplate mechanism (11, 12) involving proteins encoded by the two biosynthetic operons *pchDCBA* and *pchEFGHI* (13, 14). Pch biosynthesis is autoregulated by a positive-feedback loop (14) requiring the transcriptional regulator PchR together with Pch as an effector molecule (15, 16).

In the extracellular medium Pch chelates Fe^{3+} with a 2:1 (Pvd:Fe^{3+}) stoichiometry (10, 17, 18), with one molecule of Pch tetradentately coordinated to Fe^{3+} and the second molecule bound bidentately to complete the octahedral geometry (19). Pch has poor water solubility, and its Fe^{3+} affinity was determined in ethanol as 2×10^5 M (10). This is low compared with other siderophores, and it is possible that in aqueous solution at physiological pH the affinity for iron is higher. Once loaded with Fe^{3+}, Pch is recognized at the cell surface of *P. aeruginosa* and transported into the periplasm by a specific outer membrane transporter, FptA. The structure of this protein (20) is typical of this class of transporters; a transmembrane 22-β-stranded barrel occluded by an N-terminal domain containing a mixed four-stranded β-sheet. The Pch binding pocket is principally composed of hydrophobic and aromatic residues, con-

* This work was supported by the CNRS, the association Vaincre la Mucoviscidose (French Association against Cystic Fibrosis), Agence Nationale de Recherche Grant ANR-05-JCJC-0181-01, and Swiss National Science Foundation for Scientific Research Project 31-113955/1).

The nucleotide sequence(s) reported in this paper has been submitted to the GenBank™/EBI Data Bank with accession number(s) FJ641192.

[1] To whom correspondence should be addressed: Métaux et Microorganismes, Chimie, Biologie et Applications, ESBS, CNRS-Université de Strasbourg, FRE3211, Blvd. Sébastien Brant, BP 10412, F-67413 Illkirch, Strasbourg, France. Tel.: 33-3-90-24-47-19; Fax: 33-3-90-24-48-29; E-mail: schalk@esbs.u-strasbg.fr.

[2] The abbreviations used are: Pch, pyochelin; NeoPch, neopyochelin; EPch, enantio-pyochelin; CCCP, carbonyl cyanide *m*-chlorophenylhydrazone.

sistent with the hydrophobicity of this siderophore. In the x-ray FptA structure, a Fe-Pch complex was found in the binding site of FptA, where Pch provided a tetradentate coordination of iron. Ethylene glycol, originating from the purification procedure, provided the remaining bidentate coordination (20). The presence of such a complex in the x-ray FptA structure showed that one molecule of Pch is sufficient for a ferric Pch complex to be recognized by the transporter. The second chelator providing the remaining bidentate coordination does not interact with the transporter and can, therefore, be a different molecule, *e.g.* the siderophore cepabactin, which was found in such a ternary complex (21, 22).

Recently it was shown that *Pseudomonas fluorescens* CHA0 produces the siderophore enantio-pyochelin (EPch, see Fig. 1), the optical antipode of Pch (23). EPch was found to promote growth under iron-limiting conditions in *P. fluorescens* and to act as an inducer of its own biosynthetic genes (23), thus resembling Pch, which is both a siderophore and a signaling molecule in *P. aeruginosa* (14, 18). However, EPch did not promote growth in *P. aeruginosa* and neither did Pch in *P. fluorescens* (23), suggesting that both the EPch- and Pch-mediated iron uptake machineries are highly stereospecific in the two species. Fe-EPch is transported in *P. fluorescens* CHA0 by a homolog of the *P. fluorescens* Pf-5 transporter PFL_3498, which we have named FetA (23). Sequence comparison between FptA of *P. aeruginosa* and FetA of *P. fluorescens* showed that the two receptors are not closely related and that the amino acids interacting with Pch in the crystallized FptA receptor (20) are not conserved in FetA. We, thus, wondered whether FptA and FetA would be able to interact with the siderophore of the other species.

Using ^{55}Fe, we show here that both receptors, FptA and FetA, are highly stereoselective and do not bind and transport the ferrisiderophore of the other species. We also show by growth promotion experiments that the preference of *P. aeruginosa* and *P. fluorescens* for Pch and EPch, respectively, can be inverted by swapping the siderophore uptake systems between the two species. From our docking experiments on the FptA structure and from binding assays, we conclude that the stereospecificity of the FptA-Pch interaction relies to a large extent on the stereochemical configuration at the chiral centers C2″ and C4″, whereas the conformation at C4′ is less important.

EXPERIMENTAL PROCEDURES

Chemicals—Pch, neopyochelin (NeoPch), and EPch were synthesized and purified according to previously published protocols (23, 24). Carbenicillin disodium salt was provided from Euromedex. The protonophore carbonyl cyanide *m*-chlorophenylhydrazone (CCCP) was purchased from Sigma. $^{55}FeCl_3$ was obtained from PerkinElmer Life Sciences with a specific activity of 93.76 Ci/g. This radioactive ^{55}Fe solution was diluted with nonradioactive iron to 9.4 Ci/g. Siderophore-^{55}Fe complexes (^{55}Fe-Pch, ^{55}Fe-NeoPch, or ^{55}Fe-EPch) were prepared at concentrations of 10 μM ^{55}Fe with a siderophore:iron (mol:mol) ratio of 20:1. The solutions were prepared using a 10 mM solution of siderophores (in methanol). To 20 μl of these solutions were added 40 μl of a solution of $^{55}FeCl_3$ (250 μM, 9.4 Ci/g in HCl, 0.5 N), obtained by dilution of the stock solution. The mixtures were incubated 15 min at room temperature before the addition of 940 μl of 50 mM Tris-HCl (pH 8.0).

Media and Growth Conditions—Bacteria were routinely grown on nutrient agar and in nutrient yeast broth or LB (25, 26) at 37 °C (*P. aeruginosa* and *Escherichia coli*) or 30 °C (*P. fluorescens*). When *P. fluorescens* and *P. aeruginosa* cells were used for binding and iron uptake assays, growth occurred in succinate medium (composition was 6.0 g/liter K_2HPO_4, 3.0 g/liter KH_2PO_4, 1.0 g/liter $(NH_4)_2SO_4$, 0.2 g/liter $MgSO_4 \cdot 7H_2O$, 4.0 g/liter sodium succinate, and the pH was adjusted to 7.0 by the addition of NaOH (27)) at 30 °C. Siderophore-mediated growth promotion experiments were performed in minimal medium M9 (25) with 0.5% glycerol as a carbon source. Iron limitation was achieved in this medium by adding the iron chelator 2,2′-dipyridyl at 500 μM. Where necessary, antibiotics were added to growth media at the following concentrations: 100 μg/ml ampicillin, 100 μg/ml streptomycin, and 25 μg/ml tetracycline for *E. coli* and 100 μg/ml tetracycline for *Pseudomonas*. To counterselect *E. coli* donor cells in gene replacement experiments, chloramphenicol was used at a concentration of 10 μg/ml. Mutant enrichment was performed with tetracycline at 20 μg/ml and carbenicillin (for *P. aeruginosa*) at 2 mg/ml or cycloserine (for *P. fluorescens*) at 50 mg/ml, respectively.

Strains and Plasmids—All strains and plasmids used in this study are listed in Table 1. Gene replacement mutants were generated with suicide plasmids as described previously (28–30). Briefly, the suicide plasmids were mobilized from *E. coli* to *P. aeruginosa* or *P. fluorescens* using the helper plasmid pME497 and chromosomally integrated, with selection for tetracycline resistance. Excision of the vector via a second crossing-over was obtained by enrichment for tetracycline-sensitive cells using carbenicillin (for *P. aeruginosa*) or cycloserine (for *P. fluorescens*). The suicide plasmid pME7531 used to generate a 1025-bp deletion in the *fetA* gene (=PFL_3498 in *P. fluorescens* Pf-5) was constructed as follows. Two PCR fragments of 0.6 kilobase carrying the 3′ and 5′ ends of *fetA*, respectively, were generated from chromosomal DNA of *P. fluorescens* CHA0 using the primers rez-1 (ACGTGAATTCATGGGTAGCCGCGTTGCGC) together with rez-2 (ACGTGGATCCGATCTGGTTGACCACGCCC) and using rez-3 (ACGTGGATCCGCAATCGGAAGTGGGGGTC) together with rez-4 (ACGTAAGCTTACCAGCGATAGCGCAGGCT). Fragment 1, cleaved with EcoRI and BamHI, was ligated to BamHI- and HindIII-trimmed fragment 2 and cloned into the suicide vector pME3087 between the EcoRI and HindIII sites. Plasmid pME7531 was then introduced into *P. fluorescens* CHA400 and CHA1085 to generate the corresponding mutants CHA1080 and CHA1169, respectively.

The pyoverdine-negative *P. aeruginosa* mutant PAO6382 was obtained by deleting the *pvdF* gene in strain PAO1 using the previously described suicide plasmid pME7152 (31). All gene replacement mutants were checked by PCR.

To swap the Pch and EPch transport genes between the two *Pseudomonas* species, the genes were cloned under the control of the *lac* promoter in pME6000 as follows. The *P. aeruginosa* Pch transport genes *fptABCX* were excised from pME7036 on a 5.9-kilobase HindIII-XbaI fragment and ligated to HindIII-XbaI-cleaved pME6000 to give pME9629. To generate plasmid

TABLE 1
Strains and plasmids

Name	Relevant characteristics	Reference or source
***P. fluorescens* strains**		
CHA0	Wild type	53
CHA400	*pvd*::Tn*5*, Km^r	54
CHA1080	*pvd*::Tn*5* Δ*fetA* (=CHA0 homolog of PFL_3498), Km^r	This study
CHA1085	*pvd*::Tn*5* Δ*pchDHIEFKCBA*, Km^r	23
CHA1169	*pvd*::Tn*5* Δ*pchDHIEFKCBA* Δ*fetA*, Km^r	This study
***P. aeruginosa* strains**		
K2388	*pvd9 fptA*::ΩTc, Tc^r	22
PAD07	Δ*pvdA*:: ΩSm/Sp Δ*pchD*::Tc, Tc^r	55
PAO1	Wild type	ATCC15692
PAO6382	Δ*pvdF*	This study
PAO6383	Δ*pvdF* Δ*pchBA*	31
PAO6541	Δ*pvdF* Δ*pchBA* Δ*fptA*	31
Plasmids		
pME497	Mobilizing plasmid, Ap^r	57
pME3087	Suicide vector, ColE1 replicon, Tc^r	53
pME6000	pBBR1-based cloning vector, Tc^r	56
pME7036	pUCPSK with *fptABCX,* Ap^r	31
pME7152	pME3087 derivative carrying Δ*pvdF*	31
pME7531	pME3087 derivative carrying Δ*fetA*	This study
pME9629	pME6000 with the Pch transport genes *fptABCX* under p*lac* control	This study
pME9630	pME6000 with the EPch transport genes (CHA0 homologs of PFL_3498 to PFL_3503) under p*lac* control	This study

pME9630, the CHA0 homologs of PFL_3498 to PFL_3503, which encode FetA and a putative ABC transporter, were PCR-amplified from chromosomal DNA of CHA0 using primers XL1-ftp (ACGTGGATCCTGCTCGAGCCTGCTCCATCC) and XL1-rtp (ACGTAAGCTTTCGTTCGCCCGAAGGTTACC). The resulting 7.5- kilobase fragment was trimmed with XhoI and HindIII and cloned into pME6000, cleaved with the same enzymes.

DNA Manipulation and Sequencing—Small- and large-scale preparations of plasmid DNA were made with the QIAprep Spin Miniprep kit (Qiagen, Inc.) and Jetstar kit (Genomed GmbH), respectively. DNA fragments were purified from agarose gels with the Geneclean II kit (Bio 101, La Jolla, CA) or the MinElute and QIAquick Gel Extraction kits from Qiagen. DNA manipulations were performed according to standard procedures (25). Transformation of *E. coli*, *P. aeruginosa*, and *P. fluorescens* was carried out by electroporation (32). Sequencing was performed with the BigDye Terminator Cycle Sequencing kit and an ABI-PRISM 373 automatic sequencer (Applied Biosystems) or was carried out commercially. The DNA sequence of the *P. fluorescens* CHA0 *fetA* gene was deposited at GenBank™ under accession number FJ641192. Data base searches were conducted at NCBI using BLAST algorithms.

Ligand Binding Assays Using ^{55}Fe—The *in vivo* dissociation constants (K_d) of ^{55}Fe-Pch, ^{55}Fe-NeoPch, and ^{55}Fe-EPch complexes to FptA and FetA were determined according to the following procedure (33). PAD07 and CHA1085 cells were washed twice with an equal volume of fresh medium and resuspended in 50 mM Tris-HCl (pH 8.0) buffer at an A_{600} of 0.3 and 1.5, respectively. Cells were then first incubated for 15 min in the presence of 200 μM CCCP to avoid iron uptake and afterward for 1 h at 0 °C in a final volume of 500 μl with 0.1–200 nM ^{55}Fe-Pch, ^{55}Fe-NeoPch, or ^{55}Fe-EPch, prepared as described above under "Chemicals." The mixtures were then centrifuged at 12,000 × *g* for 2 min, and the supernatants containing the unbound siderophore-^{55}Fe were removed. The tubes containing the cell pellets were counted for radioactivity in scintillation mixture. To evaluate a nonspecific binding of ^{55}Fe-Pch, ^{55}Fe-NeoPch, or ^{55}Fe-EPch, binding experiments were repeated in parallel for each concentration of siderophore with the same strains grown in LB medium. In this iron-rich medium, neither FptA nor FetA receptors were expressed. K_d values were determined using the Scatchard representation.

Iron Uptake—Iron uptake assays were carried out as previously reported for the FptA/Pch system (22). After an overnight culture (20 h), bacteria were prepared in 50 mM Tris-HCl (pH 8.0) at A_{600} of 1 for *P. aeruginosa* or at A_{600} of 5 for *P. fluorescens* and incubated at 37 °C. Transport assays were started by adding 100 nM ^{55}Fe-Pch, ^{55}Fe-NeoPch, or ^{55}Fe-EPch prepared as described above under "Chemicals." To separate siderophore-^{55}Fe transported into *P. aeruginosa* cells from unbound siderophore-^{55}Fe, aliquots (100 μl) of the suspensions were removed at different times and filtered, and the retained radioactivity was counted in scintillation mixture. For *P. fluorescens*, aliquots (300 μl) of the cell suspensions were removed, mixed with 600 μl of cold Tris buffer, and centrifuged (12,000 × *g* for 3 min). The supernatants containing the unbound siderophore were removed, and the tubes containing the cell pellets were counted for radioactivity in scintillation mixture. This difference in the protocols used for *P. aeruginosa* cells and *P. fluorescens* cells is due to different levels of FptA and FetA expression, which led us to use much higher cell concentrations for experiments with *P. fluorescens*. As controls, the experiments were repeated with cells incubated at 0 °C in the presence of 200 μM CCCP and in the absence of cells.

Docking—Standard settings of the docking program GOLD Version4.0 (34) were used to dock Fe-PchI and Fe-EPchI. Ligand three-dimensional structures (mol2 format) were obtained from two-dimensional sketches using Marvin Sketch (ChemAxon Ltd) and further converted into three-dimensional coordinates using Corina (Molecular Networks GmbH). The iron-bound EPchI molecule assumed a tetravalent coordination of the iron atom, as seen in the FptA-bound structure of FptA (20). The FptA binding cavity was defined as any atom within a 6.5 Å radius sphere centered on the center of mass of

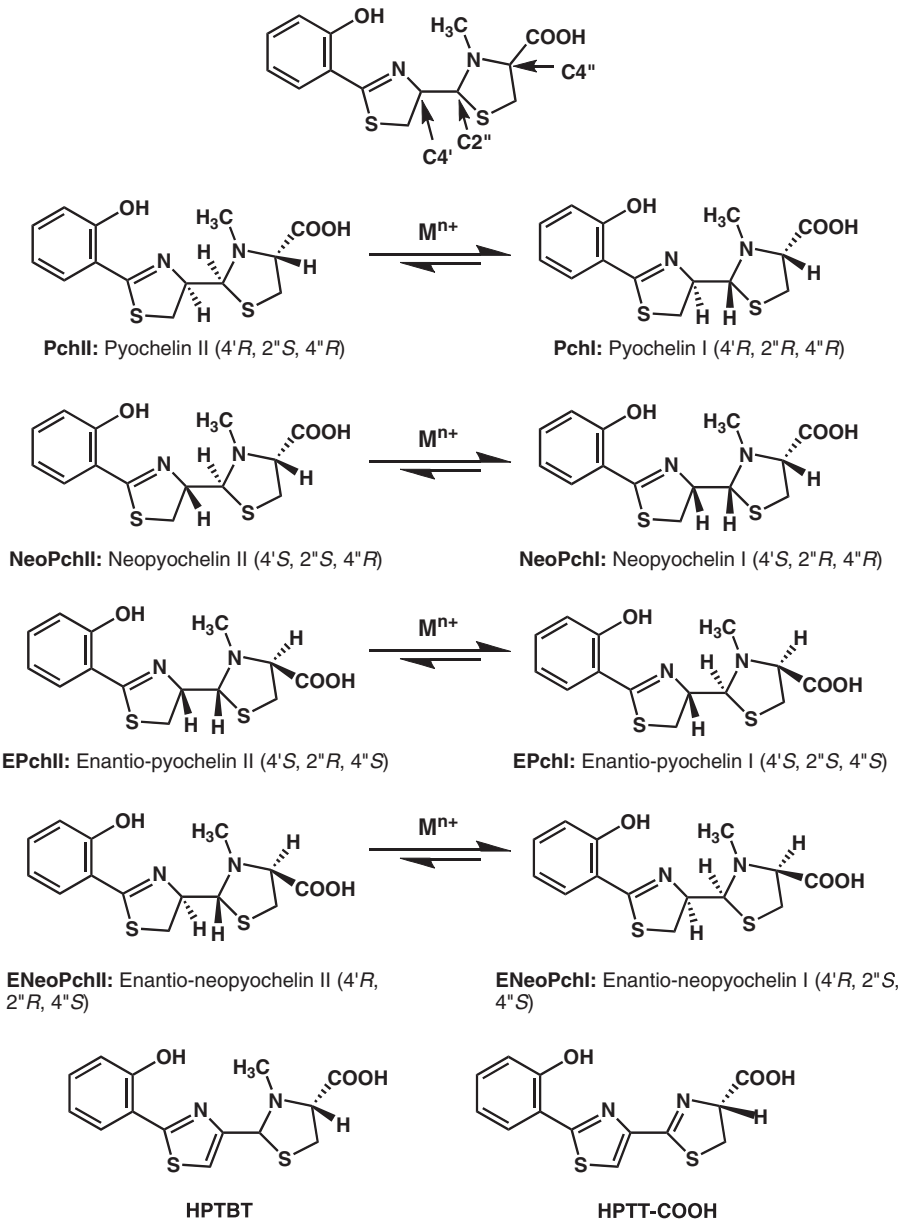

FIGURE 1. **Structures and configurations of Pch, its stereoisomers, and two analogues.** Pch contains three chiral carbons (C4′, C2″, and C4″) and can exist as four different pairs of stereoisomers (PchI/II, NeoPchI/II, EPchI/II, and ENeoPchI/II). Naturally occurring stereoisomers are PchI and -II isolated from *P. aeruginosa* PAO1 (17) and EPchI and -II made by *P. fluorescens* CHA0 (23). The metal-induced epimerization (M^{n+}) at C2″ has only been shown for Pch (17) and NeoPch (G. L. A. Mislin, and I. J. Schalk, unpublished results) but may also exist for the other stereoisomer pairs. Note that compared with the literature (23, 36), we have renamed the NeoPch and ENeoPch diastereoisomers here such that in all four isomers of type I there is now a *cis* relationship between H2″ and H4″, whereas in all isomers of type II there is now a *trans* relationship between these two hydrogen atoms.

PchI in the ptA-PchI x-ray structure (20). Docking poses were further analyzed by docking score (Goldscore), and the percentage of ligand surface was buried upon binding.

RESULTS

Binding of Pch Diastereoisomers to FptA and FetA—The specificity of iron uptake in Gram-negative bacteria is regulated at the cell surface by siderophore outer membrane transporters. These proteins are highly specific for one or a few siderophores. To investigate the binding specificities of FptA and FetA, we carried out binding assays using ^{55}Fe-loaded Pch diastereoisomers. To avoid competition with endogenous siderophores, we used the *P. aeruginosa* Pch- and Pvd-deficient strain PAD07 and the *P. fluorescens* EPch- and Pvd-deficient strain CHA1085. To measure only the binding of the siderophore-^{55}Fe to the outer membrane transporter without any uptake into the bacteria, the binding assays were carried out in the presence of the protonophore CCCP. In the presence of this compound, the siderophore outer membrane transporter is still able to bind its ferrisiderophore, but the TonB machinery and, therefore iron uptake, is inhibited. The Pch stereoisomers used for these experiments were synthesized and purified as reported previously (23, 24). The purification procedure used did not separate the diastereoisomer couples. However, in the presence of a metal ion (Fe^{3+} and Zn^{2+}), PchII isomerizes into PchI (35, 36) by epimerization of the C2″ carbon atom (Fig. 1). The thioamine function included in the thiazolidine ring can undergo ring opening and closure (37). The configuration of the C2″ carbon atom, located between the thiazolidine nitrogen and sulfur heteroatoms, is therefore highly labile, especially in the presence of a Lewis acid like a metal ion. Thus, the metal ion may drive its ligand isomerization to optimize the chelation properties through a template effect. For Pch diastereoisomers, where the hydrogen atoms H2″ and H4″ are in *cis*, the carboxylate, the thiazoline nitrogen, the thiazolidine nitrogen, and the phenol oxygen have a suitable geometry to form a tetradentate ligand of the metal. On the contrary, for the diastereoisomers where the hydrogen atoms H2″ and H4″ are in *trans*, the carboxylate is too distant from the metal to coordinate; these isomers are bare chelators. Similar metal-induced epimerization of C2″ may also occur in the other diastereoisomer pairs (Fig. 1). Therefore, the mixtures used were: PchI/II, which is PchI and PchII in the absence of iron and mainly PchI in the presence of iron; NeoPchI/II, which is NeoPchI and NeoPchII in the absence of iron and mainly NeoPchI when loaded with iron; EPchI/II, which is EPchI and EPchII in the absence of iron and mainly EPchI in the presence of iron.

TABLE 2

Dissociation constants (K_d) of siderophore-^{55}Fe to outer membrane transporters FptA and FetA determined *in vivo* at 0 °C

PAD07 (expressing FptA) and CHA1085 (expressing FetA) cells were prepared as described under "Experimental Procedures" and were incubated with a series of concentrations of ^{55}Fe-Pch or ^{55}Fe-EPch for 1 h at 0 °C. The mixtures were centrifuged, and the radioactivity in the pellet was counted. The constants were determined from a Scatchard representation, and the errors were determined from multiple Scatchard plots.

Siderophores	Outer membrane transporters	
	FptA	FetA
^{55}Fe-Pch	K_d = 2.5 nM ± 1.1	No binding observed
^{55}Fe-NeoPch	K_d = 29 nM ± 11	No binding observed
^{55}Fe-EPch	No binding observed	K_d = 3.7 nM ± 2.1

We measured binding of Pch, NeoPch, and EPch to the outer membrane receptors of *P. aeruginosa* (FptA) and *P. fluorescens* (FetA). For ^{55}Fe-Pch, a K_d of 2.5 nM ± 1.1 was determined for FptA, whereas no binding was observed to the *P. fluorescens* receptor (Table 2). Likewise, ^{55}Fe-NeoPch bound FptA, although with a 10-fold lower affinity (29 nM ± 11) than ^{55}Fe-Pch, and no binding occurred to FetA (Table 2). Binding of ^{55}Fe-NeoPch to FptA was reported previously by our group (22). However, in those experiments a siderophore preparation containing some Pch (ratio Pch/NeoPch of 3:7) was used. Our present data, obtained with a pure preparation of NeoPch, thus demonstrate clearly that NeoPch binds FptA and that the binding reported previously (22) was not only because of the presence of low amounts of Pch. ^{55}Fe-EPch bound the *P. fluorescens* receptor FetA with a K_d of 3.7 ± 2.1 nM but was unable to interact with the *P. aeruginosa* receptor (Table 2). The affinities of ENeoPch to FptA or FetA were not determined, as we do not have a sufficiently pure sample of this molecule. The concentrations of the ^{55}Fe-loaded siderophores used here were below 200 nM. At higher concentrations, an increase of radioactivity was monitored even in the absence of cells, probably because of a minor precipitation of free ^{55}Fe. Therefore, we cannot totally exclude a binding of ^{55}Fe-EPch to FptA and of ^{55}Fe-Pch to FetA with an affinity of at least 200-fold lower.

The use of a Scatchard representation to determine the affinity of a ligand for its receptor allowed us to estimate the receptor concentration. According to our experimental data, the concentrations in an overnight culture (A_{600} of 1) are 13.4 nM for FptA in *P. aeruginosa* PAD07 and 0.15 nM for FetA in *P. fluorescens* CHA1085. There is, thus, an unexplained 100-fold difference in receptor expression between the two species.

Ability of Pch Stereoisomers to Transport ^{55}Fe in P. aeruginosa and P. fluorescens—The ability of the Pch stereoisomers to transport iron in *P. aeruginosa* and *P. fluorescens* was measured with ^{55}Fe (Fig. 2). Cells were incubated in the presence of the siderophore-^{55}Fe complexes, and the amount of transported ^{55}Fe was monitored. As controls, all experiments were repeated under conditions when iron uptake is inhibited, such as in the presence of the protonophore CCCP at 0 °C or in the absence of cells (data not shown). To avoid ^{55}Fe uptake by endogenous siderophores, we used, in the case of *P. aeruginosa*, the Pch- and Pvd-deficient PAD07 strain (Fig. 2*A*). The data obtained clearly showed that PAD07 was able to transport ^{55}Fe-Pch and, with a lower uptake rate, also ^{55}Fe-NeoPch. However, no iron uptake

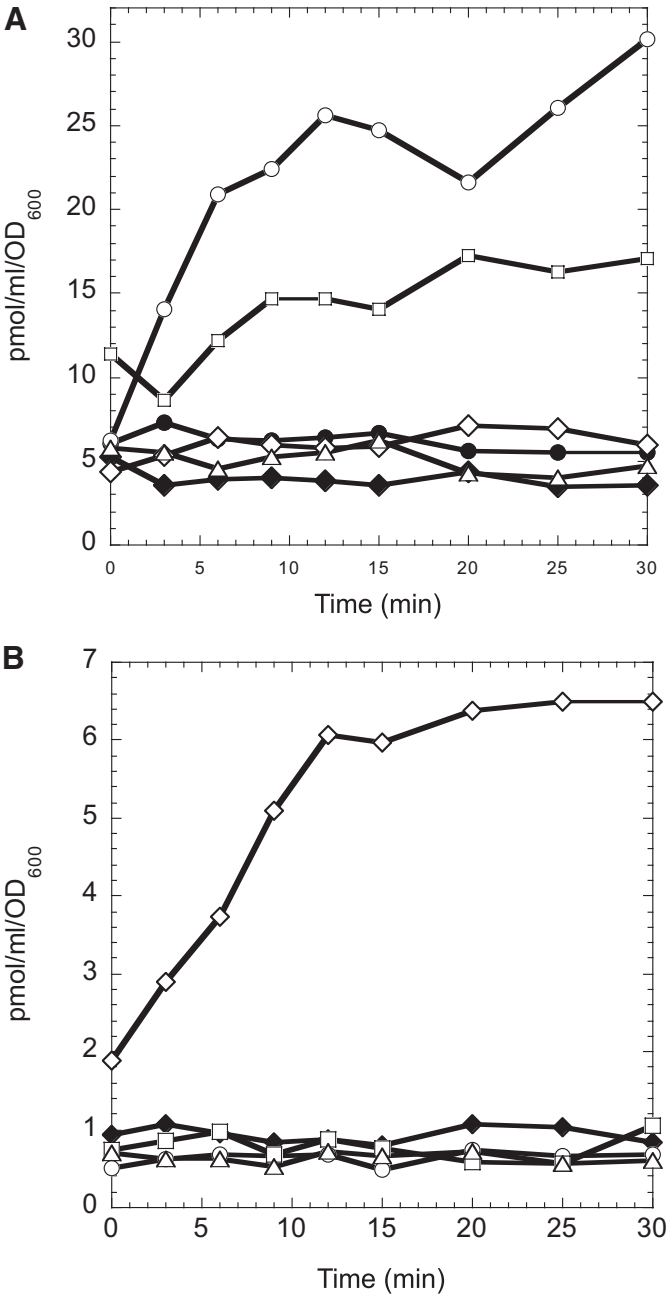

FIGURE 2. **Pch-^{55}Fe, NeoPch-^{55}Fe, and EPch-^{55}Fe uptake by *P. aeruginosa* and *P. fluorescens* strains.** *A*, after 20 h of culture, cells of *P. aeruginosa* PAD07 (Pch$^-$ and Pvd$^-$) and K2388 (Pvd$^-$ and FptA$^-$) at an A_{600} of 1 were incubated at 37 °C for 15 min in 50 mM Tris-HCl (pH 8.0) before transport assays were started by the addition of 100 nM ^{55}Fe-Pch (○ and △ for, respectively, PAD07 and K2388), ^{55}Fe-NeoPch (□ for PAD07, data not shown for K2388), or ^{55}Fe-EPch (◇ ç for PAD07, data not shown for K2388). The experiments were repeated at 0 °C in the presence of 200 μM CCCP (● for ^{55}Fe-Pch, ♦ for ^{55}Fe-EPch, and data not shown for ^{55}Fe-NeoPch) and in the absence of cells (data not shown). *B*, after 20 h of culture, cells of *P. fluorescens* CHA400 (Pvd$^-$) and CHA1080 (Pvd$^-$ and FetA$^-$) at an A_{600} of 5 were incubated at 37 °C for 15 min in 50 mM Tris-HCl (pH 8.0) before transport assays were started by the addition of 100 nM ^{55}Fe-Pch (○ for CHA400, data not shown for CHA1080), ^{55}Fe-NeoPch (□ for CHA400, data not shown for CHA1080), or ^{55}Fe-EPch (◇ and △ for, respectively, CHA400 and CHA1080). The experiments were repeated at 0 °C in the presence of 200 μM CCCP (data are shown only for CHA400 with ^{55}Fe-EPch (♦)) and in the absence of cells (data not shown).

occurred with ^{55}Fe-EPch. When the *fptA* mutant strain K2388 was used, no uptake of ^{55}Fe-Pch and ^{55}Fe-NeoPch occurred, demonstrating that the incorporation of both iron-loaded sid-

erophores occurs via FptA. All these uptake assays were carried out with 20-h cultures of *P. aeruginosa*.

When a Pvd- and EPch-deficient *P. fluorescens* strain was used (CHA1085), no ^{55}Fe uptake in the presence of ^{55}Fe-EPch was detected with cells grown for 20 h, and only a very modest uptake occurred with cells from a 48-h culture (data not shown). As mentioned above, the concentration of FetA in *P. fluorescens* was found to be considerably lower at a given optical density than the concentration of FptA in *P. aeruginosa*. Moreover, we suspect that *fetA* expression may require EPch, thus resembling the regulation of *fptA* by PchR and Pch in *P. aeruginosa* (16). It is, thus, possible that the FetA concentration was too low in the EPch-negative strain CHA1085 to detect iron uptake with ^{55}Fe-EPch under the experimental conditions used. We, therefore, performed the experiments with the Pvd-negative but EPch-producing strain CHA400 and its *fetA*-negative derivative CHA1080 (Fig. 2*B*). With CHA400 cells from a 20-h culture, ^{55}Fe-EPch but not ^{55}Fe-Pch was able to transport ^{55}Fe. ^{55}Fe-EPch uptake was abolished in the Pvd-negative Δ*fetA* mutant CHA1080, demonstrating that EPch-mediated iron uptake depends on the FetA receptor.

In *P. aeruginosa* PAD07, 30 pmol of ^{55}Fe/ml (A_{600}) were transported after 30 min in the presence of Pch. When the same experimental conditions were used with *P. fluorescens* CHA400 cells, the uptake rate of ^{55}Fe/ml (A_{600}) was only 7 pmol with EPch. This difference cannot be because of a difference in the affinities of the transporters for their respective siderophore (Table 2) but probably reflects the lower expression level of FetA in *P. fluorescens* compared with the expression of FptA in *P. aeruginosa*. Previous studies have shown that more transporters than TonB proteins are produced. A 10-fold excess was reported for the ferrichrome transporter FhuA and the enterobactin transporter FepA of *E. coli* (38–41). As TonB is required for ferric-siderophore uptake across the outer membrane, only a small amount of the transporters can be active. Therefore, a 100-fold lower expression of FetA compared with FptA does not involve a proportional decrease in the ^{55}Fe uptake rates.

Role of the Outer Membrane Receptors in Enantiospecific Growth Promotion with Pch and EPch—We evaluated the role of FptA and FetA in Pch and EPch utilization in *P. aeruginosa* and *P. fluorescens* during cell growth. As shown in Fig. 3, *B* and *G*, unmodified M9-glycerol medium contained sufficient iron to support the growth of *P. fluorescens* CHA1085 (Pvd$^-$, EPch$^-$) and *P. aeruginosa* PAO6383 (Pvd$^-$, Pch$^-$), but when the iron chelator 2,2-dipyridyl was added to the medium, these mutants were no longer able to grow. The EPch- and Pch-positive precursor strains CHA400 (Fig. 3*A*) and PAO6382 (Fig. 3*F*), respectively, grew well in the presence of the iron chelator, although CHA400 exhibited a longer lag phase. Interestingly, Pch addition delayed growth of CHA400 even more, suggesting that the heterologous siderophore Pch competes with EPch for iron. As this effect was not observed in *P. aeruginosa*, we suspect that the kinetics of siderophore production and/or receptor expression are different in the two species. Growth of the siderophore-negative *P. fluorescens* mutant CHA1085 was restored by adding 20 μM EPch (Fig. 3*B*), whereas the addition of Pch produced no such effect. Reciprocally, Pch promoted

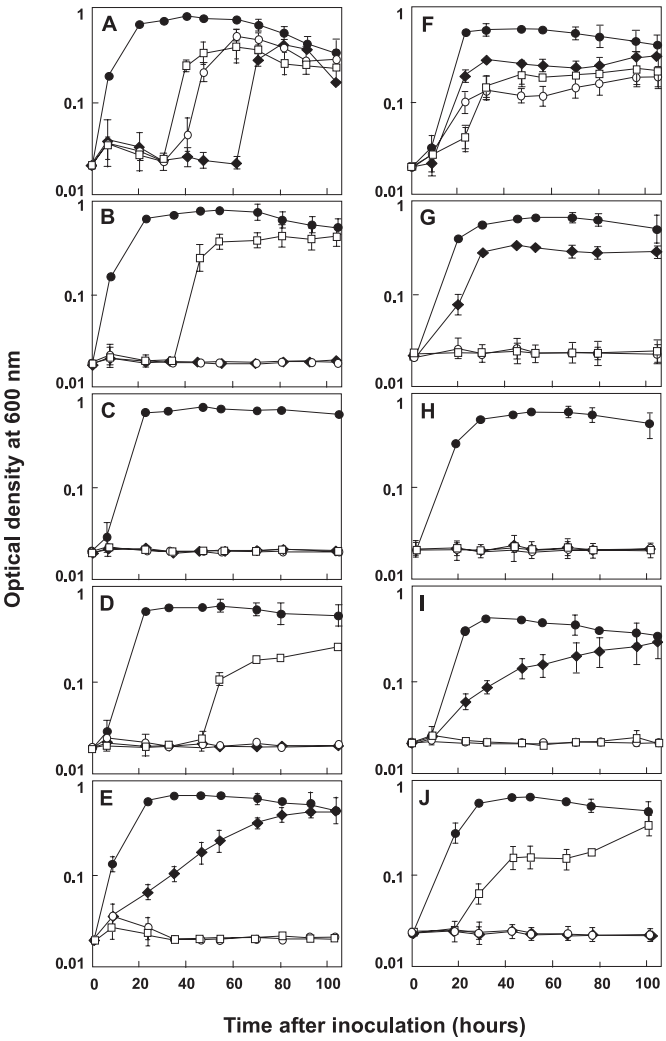

FIGURE 3. **Role of the Pch and EPch uptake genes in stereospecific siderophore-mediated growth promotion.** The *P. fluorescens* strains CHA400 (*A*), CHA1085 (*B*), CHA1169 (*C*), CHA1169/pME9630 (*D*), CHA1169/pME9629 (*E*) and the *P. aeruginosa* strains PAO6382 (*F*), PAO6383 (*G*), PAO6541 (*H*), PAO6541/pME9629 (*I*), and PAO6541/pME9630 (*J*) were grown in 200 μl of unmodified M9-glycerol medium (*filled circles*) or in M9-glycerol medium containing the iron chelator 2,2-dipyridyl at 500 μM (*empty circles*) and 20 μM HPLC-purified Pch (*filled diamonds*) or EPch (*empty squares*). Growth in 96-well microtiter plates was assessed over a period of 5 days. A_{600} values represent the means ± S.D. from three parallel cultures.

growth in PAO6383, but no growth promotion was achieved with EPch (Fig. 3*G*). These results, which have been reported previously (16), demonstrate that growth promotion is a stereospecific process. A mutation in *fptA* abolished Pch-mediated growth promotion in *P. aeruginosa* (Fig. 3*H* (31, 42)). Similarly, we have found here that the FetA receptor is essential for EPch utilization in *P. fluorescens* (Fig. 3*C*). Complementation of PAO6541 (Pvd$^-$, Pch$^-$, FptA$^-$) with the Fe-Pch uptake operon (*fptABCX*) carried by pME9629 fully restored Pch-mediated growth promotion (Fig. 3*I*), and heterologous expression of *fptABCX* in the siderophore-negative *fetA* mutant CHA1169 enabled this strain to grow with Pch instead of EPch as an iron source (Fig. 3*E*). Reciprocally, the fetA mutation of CHA1169 was complemented by pME9630, a plasmid constitutively expressing *fetA* and adjacent genes specifying a putative ABC transporter (Fig. 3*D*). When pME9630 was introduced into the

TABLE 3
Predicted binding mode of FptA ligands by Gold automated docking

Ligand	Goldscore[a]	r.m.s.d.[b]	H-bonds[c]		BSA[d]
			L116:N	L117:N	
Fe-PchI	63.81	0.30		X	97.5
Fe-NeoPchI	52.57		X		94.5
Fe-EPchI	48.72				82.3

[a] Goldscore is the fitness function of the GOLD program (34), which quantifies protein-ligand interactions according to four terms: protein-ligand H-bond interaction energy, protein-ligand van der Waals interaction energy, ligand internal van der Waals energy, ligand torsional strain energy. The data concerning Fe-NeoPchI have been published previously (22).
[b] Root mean square deviations (in Å) of the heavy atoms from the x-ray configuration of Fe-PchI.
[c] Possible H-bonds are indicated by an X.
[d] Buried surface area (in percentage of the total surface) of the FptA-bound ligand.

fptA mutant PAO6541, growth promotion occurred with EPch, whereas Pch was not utilized (Fig. 3*J*). These experiments, thus, confirm and extend the results from the above binding and ^{55}Fe uptake assays. They show that FptA and FetA are able to discriminate between the two siderophore enantiomers and that the preference of *P. aeruginosa* and *P. fluorescens* for Pch and EPch, respectively, can be inverted by swapping the respective ferrisiderophore transport genes between the two species.

Ligand Docking—To better understand the interaction mechanism of the FptA binding site with the Pch stereoisomers, we carried out docking experiments using the x-ray structure of FptA loaded with Fe-PchI (20) (Fig. 1). The program GOLD (Genetic Optimization for Ligand Docking) (34), a genetic algorithm for docking flexible ligands into protein binding sites, was used to dock all herein investigated ligands. Using automated docking, we obtained a Fe-Pch conformation very close to that of its x-ray structure (root mean square deviations of 0.3 Å from the heavy atoms) and with a high Goldscore of 63.8 (Table 3). The docking of Fe-NeoPch has been described previously and gave similar results (22). Docking of Fe-EPchI afforded quite different results. First, the docking score obtained for that compound (48.72) is significantly lower than that computed for Fe-PchI (63.81, Table 3). Second, the predicted binding mode of Fe-EPchI to FptA involves only apolar contacts with the hydrophobic binding pocket. Contrary to Fe-PchI, no hydrogen bond to the receptor could be proposed for any possible docking solution of Fe-EPchI. As a consequence, there is no strong directionality for anchoring Fe-EPchI to the FptA binding pocket, which could explain the herein reported absence of detectable affinity for the latter siderophore. A structural explanation to the absence of hydrogen bonds lies in the inverted configuration of the C4″ carbon atom, which expels the carboxylate moiety away from the binding pocket, as noticed by the decreased buried surface area of Fe-EPchI with respect to that of Fe-PchI (Table 3).

DISCUSSION

Under iron limitation, *P. aeruginosa* produces the two diastereoisomers PchI and PchII, whereas some *P. fluorescens* strains are known to produce the optical antipodes, EPchI and EPchII. The four other diastereoisomers, NeoPchI/II and ENeoPchI/II, have so far never been isolated from any siderophore-producing strain. In the presence of a metal ion, PchII isomerizes into PchI (24, 36), and NeoPchII isomerizes into NeoPchI. This suggests a metal-driven template effect giving a *cis* H2″-H4″ relationship that is necessary for optimal ferric ion tetracoordination by the siderophore. Such an isomerization may also exist for the two other couples of diastereoisomers. This isomerization suggests that in the ^{55}Fe-PchI/II, ^{55}Fe-NeoPchI/II, or ^{55}Fe-EPchI/II preparations, we have, respectively, mostly ^{55}Fe-PchI, ^{55}Fe-NeoPchI, or ^{55}Fe-EPchI. Therefore, in the present work Fe-Pch, Fe-NeoPch, and Fe-EPch are considered as, respectively, Fe-PchI, Fe-NeoPchI, and Fe-EPchI.

^{55}Fe uptake assays showed that Pch is the siderophore used by *P. aeruginosa* for iron uptake and EPch is the one used by *P. fluorescens* (Fig. 2). Absolutely no ^{55}Fe incorporation was observed when *P. aeruginosa* cells were incubated in the presence of ^{55}Fe-EPch or *P. fluorescens* in the presence of ^{55}Fe-Pch. Clearly two different iron uptake pathways exist in these two species, one using only Pch and the other, EPch. The outer membrane transporters involved are, respectively, FptA for Fe-Pch in *P. aeruginosa* and FetA for Fe-EPch in *P. fluorescens*. When their corresponding genes were mutated, ^{55}Fe-Pch and ^{55}Fe-EPch uptakes were abolished in *P. aeruginosa* and *P. fluorescens*, respectively. The use of the protonophore CCCP demonstrated that the two uptake pathways, Fe-Pch via FptA and Fe-EPch via FetA, are TonB-dependent; inhibition of the protonmotive force abolished iron uptake. The ability of FptA and FetA to discriminate between the two siderophore enantiomers was also observed in growth promotion assays (Fig. 3), and the siderophore preference of *P. aeruginosa* and *P. fluorescens* could be inverted by swapping the ferrisiderophore transport genes between the two species. The Scatchard representation allowed us to determine a K_d of 2.5 nM ± 1.1 for the binding of ^{55}Fe-Pch to FptA and a K_d of 3.7 nM ± 2.1 for the binding of ^{55}Fe-EPch to FetA (Table 2). Both K_d values are, thus, very similar to each other and to the K_d values determined for other ferrisiderophores and their specific outer membrane transporters (33, 43, 44). It seems that an affinity in the nanomolar range of ferrisiderophores for their corresponding transporters is a conserved parameter during evolution. A lower affinity may not be sufficient for bacteria in their competition for iron. It is important also to point out that, consistent with ^{55}Fe uptake assays, no binding was observed between FetA and ^{55}Fe-Pch and between FptA and ^{55}Fe-EPch under these experimental conditions. If binding does exist, it clearly would occur with a much lower affinity and would probably not allow an efficient Fe^{3+} uptake.

^{55}Fe uptake and binding assays showed that FetA was unable to bind and transport ^{55}Fe-NeoPch. However, ^{55}Fe-NeoPch was bound by FptA (K_d = 29 nM ± 11) and was also incorporated into the cells, although iron uptake was not as efficient as with Pch. By analogy with these findings, we predict that ENeoPch might be able to interact with FetA but not with FptA. Future experiments will address this issue.

The previously published x-ray structure of FptA-Fe-PchI and docking experiments were used to better understand the stereoselectivity of siderophore binding. The siderophore binding pocket is mainly composed of hydrophobic and aromatic residues, consistent with the hydrophobicity of Pch. In the FptA-Fe-PchI structure, the ferric ion is hexacoordinated by

four atoms from Pch (the nitrogen atoms of the thiazoline and thiazolidine rings and the oxygen atoms of the phenol and carboxylate groups) and two oxygen atoms from ethylene glycol, with a 1:1:1 stoichiometry (20). The observed diastereoisomer of Pch in the FptA structure is PchI. Previous docking experiments predict that Fe-PchI and Fe-NeoPchI adopt the same conformation when bound to FptA, whereas the receptor-bound conformation of Fe-PchII and Fe-NeoPchII are incompatible with strong metal chelation because of a *trans* relationship between the H2″ and H4″ protons repelling the carboxylic acid moiety far from the iron coordination sphere (22). For Fe-PchI and Fe-NeoPchI, the phenol moiety is predicted to bind similarly to a hydrophobic subsite (Tyr-356, Phe-358, Ala-144, Leu-117), and the two five-member heterocycles face the central non-polar part of the binding site (Met-271, Tyr-334, Trp-702). However, the carboxylate moiety is proposed to H-bond to two different polar environments, the Leu-116 and Leu-117 backbone nitrogen atoms (22). Docking of Fe-EPchI gave a low docking score (Table 3), suggesting that the Pch enantiomer cannot be recognized by FptA. The predicted binding mode involves only apolar contacts with the hydrophobic binding site (Fig. 4). These different docking predictions are fully consistent with our binding data on the ability of FptA to interact with the different Pch diastereoisomers (Table 2).

NeoPchI only differs from PchI by the stereochemistry of the C4′ chiral center. Because both Fe-Pch and Fe-NeoPch are able to bind to FptA with only a 10-fold difference in affinity, the configuration of the C4′ chiral center seems less important for the interaction with the transporter. Moreover, when the chiral center C4′ is removed by replacing the thiazoline moiety by a thiazole ring in hydroxy-phenyl-thiazolyl-bishydro-thiazole (HPTBT) (Fig. 1), only a slight decrease in the affinity for FptA is observed, and the iron transport properties of Fe-hydroxy-phenyl-thiazolyl-bishydro-thiazole resemble those of Fe-Pch (22). In contrast, the conformation of C4″ appears to be more critical for the interaction of Pch with FptA. When Fe-EPchI was docked in the FptA binding site, the inverted configuration of the C4″ carbon expelled the carboxylate moiety from the binding pocket, and the hydrogen-bond with Leu-116 and Leu-117 was no longer possible (Fig. 4). The absence of this hydrogen-bond may explain why there is no binding of Fe-EPch to FptA. Concerning the last chiral center, C2″, an epimerization occurs in the presence of metal for an optimal ferric ion tetracoordination by the siderophore (17, 36). In the case of Pch, this chiral center may always have the configuration *R* when loaded with metal and bound to FptA, whatever the configuration of the two other chiral centers may be. To illustrate the importance of this chiral center C2″ in the interaction of FptA with its siderophore, it is interesting to remember the biological properties of hydroxy-phenyl-thiazolyl-thiazole (HPTT-COOH) (Fig. 1). In this molecule the C4′ and C2″ chiral centers have been removed. As a consequence, the ferric-siderophore became more rigid, its affinity for FptA was slightly decreased, and it was no longer translocated across the outer membrane (22). Although Fe-hydroxyphenylthiazolylthiazole-COOH could be docked into the binding site with a score very similar to Fe-PchI, we predicted a complete inversion of the binding mode to FptA. Taken together, all these data clearly suggest

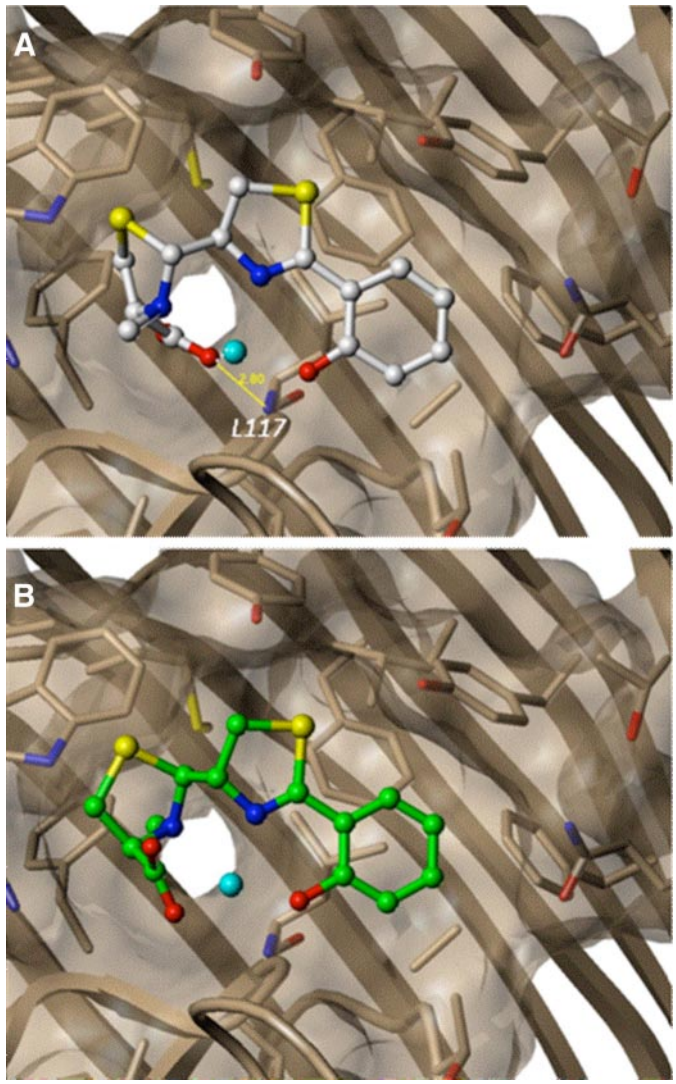

FIGURE 4. **Binding mode of Fe-PchI (x-ray structure) and Fe-EPchI (docked models) in the FptA binding site.** The most favorable docking pose of Fe-EPchI (*panel B*), obtained by the GOLD docking program (34), is displayed in the FptA binding site (residues lining the cavity are represented as *sticks*) and compared with the x-ray structure of FptA complexed with Fe-PchI (*panel A*). The accessible surface of the Pch cavity is represented by a transparent surface, and the main chain atoms of the FptA protein are displayed as a *ribbon*. Hydrogen bonds of the ligands to FptA are indicated by a *yellow solid line* with the corresponding distance in Å between interacting heavy atoms. The iron atom of the ferrisiderophores is displayed as a *cyan ball*.

that the configuration of the chiral centers C2″ and C4″ are important for the binding and uptake of Fe-Pch by FptA, whereas the configuration of the C4′ carbon atom has nearly no influence.

The mechanism of interaction between proteins and chiral ligands is a fascinating topic in biology. Stereospecificity of iron uptake systems has been observed previously with several other siderophores such as parabactin, rhodotorulic acid, ferrichrome, and enterobactin and their corresponding enantiomers (45–52). However, so far no siderophore outer membrane transporters have been described with opposite binding enantioselectivities. FptA and FetA are the first transporters with such properties; FptA is specific to Fe-Pch, and FetA is specific to the enantiomer siderophore, Fe-EPch. The investigation of the FptA binding properties allowed us to show that

the configuration of the chiral centers C2″ and C4″ are important for the binding and uptake of Fe-Pch by this transporter, whereas the configuration of the C4′ carbon atom has nearly no influence. Further studies are currently undertaken to determine the FetA-Fe-EPchI structure and to understand the mechanism driving enantioselectivity of this transporter.

REFERENCES

1. Braun, V. (2003) *Front. Biosci.* **8,** 1409–1421
2. Postle, K., and Kadner, R. J. (2003) *Mol. Microbiol.* **49,** 869–882
3. Wiener, M. C. (2005) *Curr. Opin. Struct. Biol.* **15,** 394–400
4. Castignetti, D. (1997) *Curr. Microbiol.* **34,** 250–257
5. Darling, P., Chan, M., Cox, A. D., and Sokol, P. A. (1998) *Infect. Immun.* **66,** 874–877
6. Phoebe, C. H., Jr., Combie, J., Albert, F. G., Van Tran, K., Cabrera, J., Correira, H. J., Guo, Y., Lindermuth, J., Rauert, N., Galbraith, W., and Selitrennikoff, C. P. (2001) *J. Antibiot.* (*Tokyo*) **54,** 56–65
7. Sokol, P. A. (1986) *J. Clin. Microbiol.* **23,** 560–562
8. Mossialos, D., and Amoutzias, G. D. (2007) *Future Microbiol.* **2,** 387–395
9. Liu, P. V., and Shokrani, F. (1978) *Infect. Immun.* **22,** 878–890
10. Cox, C. D., Rinehart, K. L., Jr., Moore, M. L., and Cook, J. C., Jr. (1981) *Proc. Natl. Acad. Sci. U. S. A.* **78,** 4256–4260
11. Reimmann, C., Patel, H. M., Serino, L., Barone, M., Walsh, C. T., and Haas, D. (2001) *J. Bacteriol.* **183,** 813–820
12. Crosa, J. H., and Walsh, C. T. (2002) *Microbiol. Mol. Biol. Rev.* **66,** 223–249
13. Serino, L., Reimmann, C., Visca, P., Beyeler, M., Chiesa, V. D., and Haas, D. (1997) *J. Bacteriol.* **179,** 248–257
14. Reimmann, C., Serino, L., Beyeler, M., and Haas, D. (1998) *Microbiology* **144,** 3135–3148
15. Heinrichs, D. E., and Poole, K. (1993) *J. Bacteriol.* **175,** 5882–5889
16. Michel, L., Gonzalez, N., Jagdeep, S., Nguyen-Ngoc, T., and Reimmann, C. (2005) *Mol. Microbiol.* **58,** 495–509
17. Ankenbauer, R. G., Toyokuni, T., Staley, A., Rinehart, K. L., Jr., and Cox, C. D. (1988) *J. Bacteriol.* **170,** 5344–5351
18. Cox, C. D. (1980) *J. Bacteriol.* **142,** 581–587
19. Tseng, C. F., Burger, A., Mislin, G. L. A., Schalk, I. J., Yu, S. S.-F., Chan, S. I., and Abdallah, M. A. (2006) *J. Biol. Inorg. Chem.* **11,** 419–432
20. Cobessi, D., Celia, H., and Pattus, F. (2005) *J. Mol. Biol.* **352,** 893–904
21. Klumpp, C., Burger, A., Mislin, G. L., and Abdallah, M. A. (2005) *Bioorg. Med. Chem. Lett.* **15,** 1721–1724
22. Mislin, G. L. A., Hoegy, F., Cobessi, D., Poole, K., Rognan, D., and Schalk, I. J. (2006) *J. Mol. Biol.* **357,** 1437–1448
23. Youard, Z. A., Mislin, G. L., Majcherczyk, P. A., Schalk, I. J., and Reimmann, C. (2007) *J. Biol. Chem.* **282,** 35546–35553
24. Zamri, A., and Abdallah, M. A. (2000) *Tetrahedron* **56,** 249–256
25. Sambrook, J., and Russel, D. W. (2001) *Molecular Cloning: A Laboratory Manual*, Cold Spring Harbor Laboratory, Cold Spring Harbor, NY
26. Stanisich, V. A., and Holloway, B. W. (1972) *Genet. Res.* **19,** 91–108
27. Demange, P., Wendenbaum, S., Linget, C., Mertz, C., Cung, M. T., Dell, A., and Abdallah, M. A. (1990) *Biol. Metals* **3,** 155–170
28. Laville, J., Blumer, C., Von Schroetter, C., Gaia, V., Defago, G., Keel, C., and Haas, D. (1998) *J. Bacteriol.* **180,** 3187–3196
29. Schnider, U., Keel, C., Blumer, C., Troxler, J., Defago, G., and Haas, D. (1995) *J. Bacteriol.* **177,** 5387–5392
30. Ye, R. W., Haas, D., Ka, J. O., Krishnapillai, V., Zimmermann, A., Baird, C., and Tiedje, J. M. (1995) *J. Bacteriol.* **177,** 3606–3609
31. Michel, L., Bachelard, A., and Reimmann, C. (2007) *Microbiology* **153,** 1508–1518
32. Farinha, M. A., and Kropinski, A. M. (1990) *FEMS Microbiol. Lett.* **58,** 221–225
33. Hoegy, F., Celia, H., Mislin, G. L., Vincent, M., Gallay, J., and Schalk, I. J. (2005) *J. Biol. Chem.* **280,** 20222–20230
34. Verdonk, M. L., Cole, J. C., Hartshorn, M. J., Murray, C. W., and Taylor, R. D. (2003) *Proteins* **52,** 609–623
35. Barnard, T. J., Watson, M. E., and McIntosh, M. A. (2001) *Mol. Microbiol.* **41,** 527–536
36. Rinehart, K. L., Staley, A. L., Wilson, S. R., Ankenbauer, R. G., and Cox, C. D. (1995) *J. Org. Chem.* **60,** 2786–2791
37. Schlegel, K., Taraz, K., and Budzikiewicz, H. (2004) *Biometals* **17,** 409–414
38. Ecker, D. J., Matzanke, B. F., and Raymond, K. N. (1986) *J. Bacteriol.* **167,** 666–673
39. Greenwald, J., Hoegy, F., Nader, M., Journet, L., Mislin, G. L. A., Graumann, P. L., and Schalk, I. J. (2007) *J. Biol. Chem.* **282,** 2987–2995
40. Higgs, P. I., Larsen, R. A., and Postle, K. (2002) *Mol. Microbiol.* **44,** 271–281
41. Kadner, R. J., and Heller, K. J. (1995) *J. Bacteriol.* **177,** 4829–4835
42. Ankenbauer, R. G., and Quan, H. N. (1994) *J. Bacteriol.* **176,** 307–319
43. Newton, S. M., Igo, J. D., Scott, D. C., and Klebba, P. E. (1999) *Mol. Microbiol.* **32,** 1153–1165
44. Schalk, I. J., Hennard, C., Dugave, C., Poole, K., Abdallah, M. A., and Pattus, F. (2001) *Mol. Microbiol.* **39,** 351–360
45. Bergeron, R. J., Dionis, J. B., Elliott, G. T., and Kline, S. J. (1985) *J. Biol. Chem.* **260,** 7936–7944
46. Bergeron, R. J., Xin, M. G., Weimar, W. R., Smith, R. E., and Wiegand, J. (2001) *J. Med. Chem.* **44,** 2469–2478
47. Drechsel, H., Jung, G., and Winkelmann, G. (1992) *Biometals* **5,** 141–148
48. Muller, G., Isowa, Y., and Raymond, K. N. (1985) *J. Biol. Chem.* **260,** 13921–13926
49. Münzinger, M., Taraz, K., Budzikiewicz, H., Drechsel, H., Heymann, M., Winkelmann, G., and Meyer, J.-M. (1999) *Biometals* **12,** 189–193
50. Neilands, J. B., Erickson, T. J., and Rastetter, W. H. (1981) *J. Biol. Chem.* **256,** 3831–3832
51. Winkelmann, G. (1979) *FEBS Lett.* **97,** 43–46
52. Winkelmann, G., and Braun, V. (1981) *FEMS Microbiol. Lett.* **11,** 237–241
53. Voisard, C., Bull, C., Keel, C., Laville, J., Maurhofer, M., Schnider, U., Défago, G., and Haas, D. (1994) in *Molecular Ecology of Rhizosphere Microorganisms* (O'Gara, F., Dowling, D. N., and Boesten, B., eds) pp. 67–89, VCH Publishers, Inc., Weinheim, Germany
54. Keel, C., Voisard, C., Berling, C. H., Kahr, G., and Défago, G. (1989) *Phytopathology* **79,** 584–589
55. Takase, H., Nitanai, H., Hoshino, K., and Otani, T. (2000) *Infect. Immun.* **68,** 1834–1839
56. Maurhofer, M., Reimmann, C., Schmidli-Sacherer, P., Heeb, S., Haas, D., and Defago, G. (1998) *Phytopathology* **88,** 678–684
57. Blumer, C., Heeb, S., Pessi, G., and Haas, D. (1999) *Proc. Natl. Acad. Sci. U. S. A.* **96,** 14073–14078